Global Biogeochemical Cycles®

RESEARCH ARTICLE
10.1029/2022GB007484

Differential Trends in Iron Concentrations of Boreal Streams Linked to Catchment Characteristics

M. Škerlep[1,2], S. Nehzati[1,3], R. A. Sponseller[2], P. Persson[4], H. Laudon[5], and E. S. Kritzberg[1]

[1]Biology Department, Faculty of Science, Lund University, Lund, Sweden, [2]Department of Ecology and Environmental Sciences, Faculty of Science and Technology, Umeå University, Umeå, Sweden, [3]MAX IV Laboratory, Lund University, Lund, Sweden, [4]Centre for Environmental and Climate Science, Faculty of Science, Lund University, Lund, Sweden, [5]Department of Forest Ecology and Management, Swedish University of Agricultural Science, Umeå, Sweden

Abstract Increasing iron (Fe) concentrations have been reported for freshwaters across northern Europe over the last decades. This increase, together with elevated concentrations of dissolved organic carbon (DOC), leads to browning of freshwaters, which affects aquatic organisms, ecosystem functioning, biogeochemical cycles, and brings challenges to drinking water production. However, how such increasing trends in stream Fe concentrations reflect the contribution of different catchment sources remains poorly resolved. Here, we explored how catchment characteristics, that is, mires and coniferous soils, regulate spatial and temporal patterns of Fe in a boreal stream network. For this, we determined Fe speciation in riparian and mire soils, and studied temporal Fe dynamics in soil-water and stream-water over a span of 18 years. Positive Fe trends were found in the solution of the riparian soil, while no long-term trend was observed in the mire. These differences were reflected in stream-water, where three headwater streams dominated by coniferous cover also displayed positive Fe trends, whereas the mire dominated stream showed no trend. Surprisingly, the majority of higher order streams showed declining Fe trends, despite long-term increases in DOC. In addition, we found that an extreme drought event led to a prolonged release of Fe and DOC from the riparian soils, that could have long-term effects on stream Fe concentrations. Our results show that riparian forest soils can be major contributors to ongoing increases in freshwater Fe concentrations and that drought can further promote the release of Fe from organic soils.

Plain Language Summary Iron (Fe) concentrations have been increasing in many northern streams, rivers and lakes. Together with increasing organic matter concentrations this leads to water becoming browner, which has consequences for aquatic organisms and interferes with drinking water production. To better understand what causes the increase in Fe, we studied Fe trends in boreal streams and organic rich mire and forest soils, which are the main sources of Fe to aquatic systems. We found that where coniferous forest soils were the main catchment source, Fe concentrations in streams were increasing, whereas Fe concentrations did not change over time when mires were the main sources. Our results also suggest that extreme events such as drought can lead to increased release of Fe from organic forest soils to streams. This research improves our understanding of the catchment Fe sources and how they contribute to past and future Fe trends in streams.

Key Points:

- Increasing Fe trends observed in headwater streams with coniferous forest catchments, but not in streams draining a mire-dominated catchment
- Surprisingly, the majority of higher order streams showed declining Fe trends despite long-term increases in dissolved organic carbon (DOC)
- Extreme drought event led to prolonged release of Fe and DOC from riparian soils and could affect stream Fe concentrations in the long-term

Supporting Information:

Supporting Information may be found in the online version of this article.

Correspondence to:

M. Škerlep,
skerlep.martin.uni@gmail.com;
martin.skerlep@umu.se

Citation:

Škerlep, M., Nehzati, S., Sponseller, R. A., Persson, P., Laudon, H., & Kritzberg, E. S. (2023). Differential trends in iron concentrations of boreal streams linked to catchment characteristics. *Global Biogeochemical Cycles*, *37*, e2022GB007484. https://doi.org/10.1029/2022GB007484

Received 8 JUN 2022
Accepted 10 FEB 2023

Author Contributions:

Conceptualization: M. Škerlep, R. A. Sponseller, P. Persson, H. Laudon, E. S. Kritzberg
Data curation: M. Škerlep, S. Nehzati
Formal analysis: M. Škerlep, S. Nehzati
Funding acquisition: R. A. Sponseller, H. Laudon, E. S. Kritzberg
Investigation: M. Škerlep, E. S. Kritzberg
Methodology: M. Škerlep, S. Nehzati, P. Persson
Resources: H. Laudon

1. Introduction

Over the last decades, increases in surface water iron (Fe) concentrations have been observed in Europe and parts of North America (Björnerås et al., 2017; Musolff et al., 2017; Neal et al., 2008; Sarkkola et al., 2013). These Fe trends coincide with increasing dissolved organic carbon (DOC) concentrations, which together lead to greater surface water color, also known as "browning" or "brownification" (Kritzberg & Ekström, 2012). Browning has been extensively studied due to its effects on species distributions, ecosystem functioning, biogeochemical cycles, and the challenges it brings to drinking water production (Kritzberg et al., 2019; Solomon et al., 2015). The majority of studies looking at the causes of browning have focused on changes in DOC concentrations and water color (Haaland et al., 2010; Kritzberg, 2017; Monteith et al., 2007), whereas fewer have investigated what factor/s may cause the increase in Fe concentrations (Björnerås et al., 2022; Ekström et al., 2016; Neal et al., 2008). While several hypotheses have been proposed, it remains unclear what drives the increase in Fe concentrations and if this is linked to broad scale factors, such as climate and acid deposition, or reflects more local, catchment scale processes, such as changes in land cover and land use.

Software: S. Nehzati
Supervision: P. Persson, E. S. Kritzberg
Visualization: M. Škerlep, S. Nehzati
Writing – original draft: M. Škerlep
Writing – review & editing: R. A. Sponseller, P. Persson, H. Laudon, E. S. Kritzberg

Research to date points to a range of factors that may influence trends in Fe concentrations, including changes in precipitation and temperature, decreases in sulfur (S) deposition, and land cover change (Björnerås et al., 2017). For example, warmer and wetter conditions promote reductive dissolution of Fe(III) minerals in catchment soils, which may enhance export to surface waters, because ferrous iron (Fe(II)) is more soluble than ferric (Fe(III)) (Ekström et al., 2016; Sarkkola et al., 2013). Recovery from deposition-driven acidification may indirectly lead to increasing Fe concentrations by enhancing the solubility of organic matter (OM) (Neal et al., 2008), which is suppressed at low pH (Ekström et al., 2011; Monteith et al., 2007). In this context, interactions with DOC stabilize Fe in solution (Karlsson & Persson, 2012; Stumm & Morgan, 2012). The tight coupling between Fe and DOC is also the reason that soils with high organic matter content, such as organic forest and wetland soils, support high Fe concentrations in solution and act as major sources of Fe to freshwaters (Lidman et al., 2017; Palviainen et al., 2015; Sarkkola et al., 2013). Notably, coniferous (e.g., spruce) forests that build up thick organic soil layers have been identified as a particularly important source of Fe to surface waters (Maranger et al., 2006; Sarkkola et al., 2013). In parts of the northern hemisphere, coniferous forests have expanded over the last century (Fuchs et al., 2013; Lindbladh et al., 2014), which could lead to an increase in Fe available for export to surface waters. Moreover, older spruce forest stands with higher soil OM content, and lower pH, can support higher dissolved Fe concentrations, suggesting that not only expanding catchment cover but also the aging of spruce forests could enhance Fe export from forest soils (Škerlep et al., 2021).

Although several of the abovementioned studies have assessed drivers of Fe exports at catchment or regional scales, little is known about how different catchment sources (i.e., forest soils and mires) contribute to ongoing trends in surface water Fe concentrations. To the extent that Fe concentrations in streams reflect the distribution of different sources and the mobilization of DOC, temporal trends may be highly variable at the scale of stream networks. For example, spatial heterogeneity in DOC trends can reflect the small-scale distribution of peatlands (mires) with large and vulnerable OM pools (Monteith et al., 2015). By contrast, recent work in a boreal stream network showed that DOC increases were strongest in streams draining forest-dominated catchments, which were parallel to changes in riparian soil solution chemistry, whereas DOC in streams draining mires showed no trends (Fork et al., 2020). Further, the contribution of organic rich riparian soils and mires to stream Fe concentrations may vary with seasonal changes in discharge, with mires being the main source of Fe to streams during baseflow, and with greater contributions from organic forest soils during high discharge (Björkvald et al., 2008). Despite these findings, to date, no studies have explicitly tested the importance of catchment land cover to long-term Fe trends. Knowing where the trends originate is a prerequisite for any management action to try to suppress or mitigate browning.

Here, we ask how catchment characteristics, namely the contribution of forest soils and mires, shape long-term trends in stream Fe concentrations. For this, we utilize the infrastructure and long-term data records from the Krycklan Catchment Study (KCS) in Northern Sweden (Laudon, Hasselquist, et al., 2021). We compare 13 streams with differing land cover and drainage areas to test whether long-term trends in stream Fe concentration are uniform across catchments or if instead catchment components contribute disproportionally to the observed trends. We also characterize Fe pools in riparian forest and mires soils using X-ray absorption spectroscopy (XAS) and focus on understanding the dynamics of mobilization in and from these two catchment sources by analyzing soil solutions. Since mobilization and transport of Fe are tightly connected to that of DOC, we expected that Fe trends in streams would follow those of DOC and that the correlation between Fe and DOC would be strongest closest to the catchment sources and will fade further downstream.

2. Materials and Methods

2.1. Site Description

The Krycklan Catchment Study (64°14′N, 19°46′E) is located in boreal Northern Sweden approximately 50 km from the city Umeå. The climate is characterized as cold temperate humid, with an average yearly temperature of 2.0°C (1981–2020), the lowest monthly average in January (−9.2°C) and the highest in July (14.6°C). Mean annual precipitation, ca. 30% of which comes as snowfall, is 620 mm (ranging between 324 and 903 mm), with no statistical trend over the last 40 years (Laudon, Hasselquist, et al., 2021). The area is susceptible to climate change as the mean annual temperature has increased by 2.5°C in the last 40 years, most rapidly during winter months. Snow cover lasts on average 167 days (during the last 40 years) but has been decreasing at a rate of ~0.5 days per year during the period (Laudon, Hasselquist, et al., 2021).

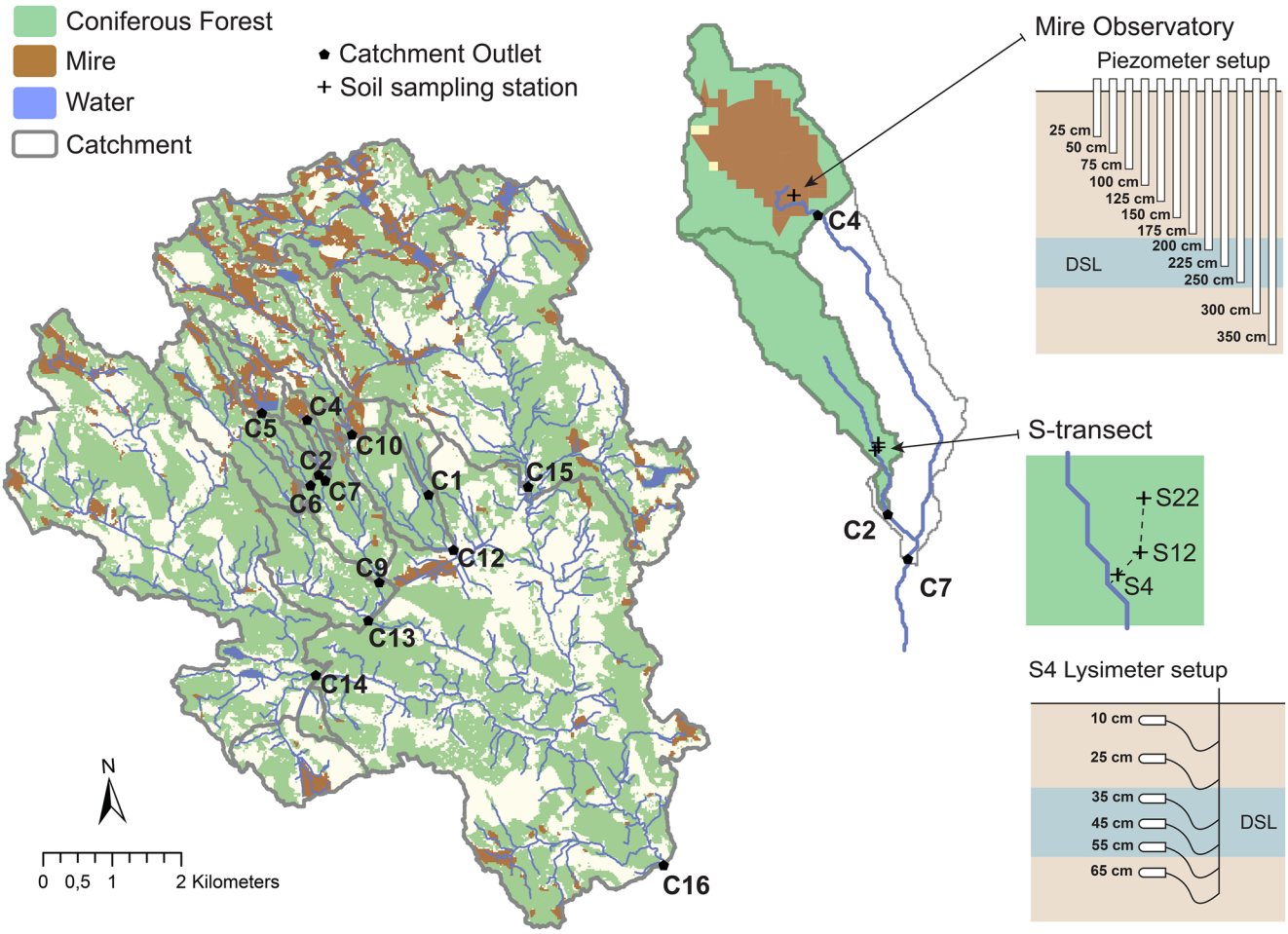

Figure 1. An overview of the land cover in the study catchments and the monitoring sites at catchment outlets. On the right, the C2 (coniferous forest dominated) and the C4 (mire dominated) catchments, as well as the soil and soil solution sampling sites in the mire and the riparian transect.

Bedrock at the site is dominated by migmatised meta-greywacke or paragneiss and has been strongly shaped by the latest glaciation. The ice retreated from the area ca. 10200 BP, leaving behind till deposits and bare bedrock in exposed areas as well as glacifluvial silt and sand deposits in the lower areas. Approximately half of the KCS was located below the highest postglacial coastline at the termination of deglaciation. Land cover in the KCS is currently dominated by forest (87%), of which 63% is Scots pine (*Pinus sylvestris*) and 26% Norway spruce (*Picea abies*) with an understory of ericaceous shrubs. Peatlands have developed in areas of lower topographic relief and are classified as oligotrophic minerogenic mires. More detailed information on the climate, geology, land use and land cover in the KCS can be found in Laudon et al. (2013) and Laudon, Hasselquist et al. (2021).

2.2. Sampling and Analysis

For this study, physicochemical monitoring data of both stream water and soil solutions from a riparian zone and a mire in the KCS were compiled for the period 2003–2020. We assessed long-term trends for 13 streams draining catchments that vary widely in land cover and size (Figure 1; Table 1). In terms of land cover, streams C2 and C4 represent the most extreme characteristics, with 100% forest cover in C2, and 44% mire and 54% forest cover in C4. Concentrations of Fe and other metals were determined using ICP-AES (ICP-MS in 2008), while DOC concentrations were determined using high-temperature catalytic-oxidation. Data on Fe concentration were available for the whole period (2003–2020) for the majority of streams, while data were limited to the period 2003–2016 for streams C10, C12, C14, and C15. To characterize the Fe pools in the forest riparian zone and mire, soil samples were collected and analyzed for Fe speciation using XAS (see Section 2.4). XAS was selected for its strengths in investigating the local atomic structure of complex natural systems due to its compatibility to

Table 1
Stream Catchment Characteristics

Stream	Area (ha)	Lake cover (%)	Forest cover (%)	Mire cover (%)	Open (%)	Arable (%)	Tree volume (m^3/ha)	Birch (%)	Spruce (%)	Pine (%)	Stand age (yr)	Till (%)	Thin soils (%)	Bedrock outcrop (%)	Sorted sediments (%)
C1	48	–	98	2	–	–	187	2	63	35	87	92	8	–	–
C2	12	–	100	–	–	–	212	0	36	64	103	84	16	–	–
C4	18	–	56	44	–	–	83	0	45	55	57	22	27	–	–
C5	65	6.4	54	40	–	–	64	12	26	62	50	40	5.5	–	–
C6	110	3.8	71	25	–	–	117	4	26	70	69	54	11	2.5	–
C7	47	0	82	18	–	–	167	1	35	64	86	65	15	0	–
C9	288	1.5	84	14	–	–	150	6	29	65	78	69	7	1.7	4
C10	336	–	74	26	–	–	93	12	21	68	60	60	11	–	1
C12	544	–	83	17	–	–	129	8	34	57	72	67	8	–	6
C13	700	0.7	88	10	0.2	0.6	145	8	25	68	78	61	9	1.3	16
C14	1410	0.7	90	5	0.9	2.9	106	10	23	67	62	45	8	1.6	38
C15	1913	2.4	82	15	1.4	0.1	85	10	26	64	54	65	8	0.7	10
C16	6790	1	87	9	1.1	1.9	106	10	26	63	62	51	7	1.2	30

measure nearly all sample-types, detection limit to trace levels, and capabilities in "seeing" all the atoms of the element of interest.

To study the contribution of coniferous forest soils to stream Fe, we took soil and soil solution samples from a riparian monitoring station just above the C2 stream sampling station. Soil samples were collected at three distances (S4 = 4 m, S12 = 12 m and S22 = 22 m) from stream C2 (Figure 1), to represent both near stream riparian soils and more upland mineral soils. S4 and S12, which are 10 and 20 cm elevated from the stream channel edge (Laudon et al., 2004), can both be considered as within the riparian zone and lack distinct soil horizons. The organic layer is 80 cm thick at S4 and 20–30 cm thick at S12. This accumulation of OM in the riparian zone is typical for headwaters in northern boreal landscapes, including the Krycklan catchment (Grabs et al., 2012). S22 is considered to be in upland soil (55 cm elevated from stream channel edge) and is characterized as an iron Podzol, with an 8 cm thick organic layer and low content of OM below 10 cm (<0.8%; Lidman et al. (2017)). Most of the water transport takes place above a compact basal till layer at a depth of ca. 1 m (Laudon et al., 2004; Peralta-Tapia et al., 2015). At each sampling point, soil samples were taken from 2 to 3 depths, corresponding to the observed layers in the soil profile (S4: 10–19, 19–35, 45–55 cm; S12: 10–20, 20–40, 40–55 cm; S22: 8–15, 20–35 cm). The upper sample at each sampling point was taken below the moss and coarse undecomposed plant litter and represented the surface organic soil layer (Oa horizon). Further data for the forest soil transect are available in Laudon et al. (2004) and Lidman et al. (2017).

To study Fe trends in the spruce forest riparian zone, soil solution chemistry data were collected 4 m from the stream (S4), using ceramic suction lysimeters (P80, UMS, Germany) installed in 1995 at 6 depths (10, 25, 35, 45, and 65 cm; Figure 1). The Dominant Source Layer (DSL) at this site, that is, the layer that provides the greatest contribution of solute and water fluxes to the stream, is between 35 and 55 cm deep (Peralta-Tapia et al., 2015). Lysimeters were sampled 2–10 times per year (5.5 time on average) during the period 2003–2020.

Solid samples were collected from the mire with a Russian corer at half-meter increments. The cores were kept intact, stored in plastic bags, and frozen immediately upon return to the field station (ca. 1 hr after sampling). From each core a subsample was taken, keeping it frozen throughout, and was freeze-dried for XAS analysis in order to remove water and concentrate the Fe. Finally, the soil solution in oligotrophic minerogenic mire, located within catchment C4, was sampled using 12 piezometers installed at depths between 25 and 450 cm (Figure 1). The DSL in the mire is located between 200 and 250 cm deep (Peralta-Tapia et al., 2015). Mire samples were analyzed for Fe during the years 2004 and 2007 as well as during the period 2017–2020.

2.3. Discharge Modeling and Flux Estimates

Discharge (Q) was measured at the outlet of each subcatchment, at the same locations where samples were collected for water chemistry (Karlsen et al., 2016). In short, automatic water-level observations from pressure loggers at each site were used to estimate stage (depth). Frequent manual water-level measurements were made to calibrate the automatic data, and stage-Q relationships were calculated for each catchment outlet using manual flow gauging. Missing data, especially during winter from stations without heated weirs were gap-filled using a semidistributed hydrological model (Karlsen et al., 2019). From the modeled daily discharge values, we calculated the Fe fluxes for each stream by linearly interpolating daily concentrations between measured values and multiplying by daily discharge. Fe fluxes are expressed as mean fluxes in kg day^{-1}.

2.4. XAS Data Collection

XAS data for riparian soil samples were collected at Stanford Synchrotron Radiation Lightsource (SSRL), beamline 4-1, California, USA. The beamline was equipped with a Si[2 2 0] double crystal monochromator, one passive implanted planar silicon detector for fluorescence measurement and had three consecutive ion chambers to monitor the incident beam as well as the beam passing through the sample and a Fe(0) reference foil. A manganese filter and Soller slits were used to reduce unwanted scattering contributions to the measured signal. Samples were mounted at 45° relative to the beam and kept frozen in a liquid nitrogen cryostat (ca. 80 K) to prevent sample damage. For each sample, 2–5 scans were recorded and recordings of the Fe(0) reference were made simultaneously for energy calibration. Fe K-edge spectra were collected up to k 13.15 $Å^{-1}$ in fluorescence mode.

X-ray data for mire soil samples were collected at the Balder beamline at the MAX IV synchrotron light facility in Lund, Sweden. The Balder beamline is equipped with a Si[111] double crystal monochromator, which was detuned to 50% to remove higher harmonics. Monochromator energy calibration was performed at the start of measurements using the first inflection point of an Fe(0) reference foil. The energy axis was monitored with repeated collection of Fe(0) reference foil spectra. Sample measurements were collected at room temperature in transmission mode using ion chambers before and after the sample position with a beam spot size of approximately 100 μm. For each sample, 99–132 scans were measured across the Fe K-edge with a data acquisition time of 1 min for each scan. The measuring position was relocated to fresh spots on the sample between each scan to prevent X-ray induced photo-damage.

2.5. XAS Data Analysis

XAS data treatment was performed using the VIPER program (Klementiev, 2001). First, all individual spectra were energy calibrated identically with a standard Fe(0) reference foil by setting the energy axis to the lowest-energy inflection point of Fe(0) reference foil at 7111.08 eV to establish a constant and accurate baseline for comparing all spectra. This energy calibration allows us to compare spectra collected at different times and at different beamlines. Following, data were normalized, averaged and background subtracted using a Bayesian smoothing spline function. A linear combination fit (LCF) was performed using least-squares optimization of model Fe spectra using the DATFIT program (George, 2000). Suwannee River fulvic acid (SRFA; 1S101 F) complexed with Fe(III) was used as a model for organically complexed Fe (Karlsson & Persson, 2012). X-ray Absorption Near Edge Structure (XANES) spectra were fit from 7,100 to 7,200 eV and Extended X-ray Absorption Fine Structure (EXAFS) spectra ranging from k 3.0 to 12.0 $Å^{-1}$ depending on the data quality. During LCF optimization, E_0 was allowed to float and components with contributions of less than 1%, after considering one standard deviation, were omitted. Preedge peaks were also fit following the method described by Wilke et al. (2001) using the Fityk program (Wojdyr, 2010). Briefly, a spline function was used to remove the baseline and isolate the preedge peak. The preedge peak was then fitted using a 50/50 pseudo-Voigt function to identify the integrated centroid and peak intensities.

2.6. Statistical Analysis

All statistical analyses were performed using RStudio version R 3.6.2 (Dark and Stormy Night). To test for trends in chemical and climatic variables in streams, the riparian forest soil and the mire, Seasonal Kendall Tests were performed in package "rkt" (Marchetto & Marchetto, 2015), and the Theil-Sen estimates of slope were calculated

to determine the rate and direction of change. In this analysis, trends are calculated for each month separately and then summed for the overall statistics. This test is robust against missing data and excludes months with less than 4 observations from the overall statistics (Hirsch & Slack, 1984). Median monthly values were used for the Seasonal Kendall Test.

To assess the impact of catchment characteristics on Fe trends, we used principal component analysis (PCA) of catchment characteristics. The PCA analysis was performed using the package "vegan" (Oksanen et al., 2013) and values were scaled to unit variance prior to analysis. The scores from the first principal component (PC1) were then correlated with the Theil-Sen slope estimates from the Seasonal Kendall Test to see how the trends in streams were related to the catchment characteristics.

To compare the relationship between Fe concentrations and chemical variables in the different systems, we used the nonparametric Kendall correlation analysis. In addition, we used linear regression to determine the intercepts and slopes of the relationships between Fe and other variables. When evaluating the effect of discharge (Q) on Fe concentrations in the streams, tests were performed using log-transformed Q values. Partial least square (PLS) analysis was performed, using the package "plsdepot" (Sanchez & Sanchez, 2012), to test the relationship between Fe and other variables in the solution of the riparian zone and the mire as well as in stream water of C2 and C4. The number of significant PLS components was determined by cross-validation and standard regression coefficients (SRC) are reported to quantify the separate contribution of each variable in explaining the variation in Fe concentrations. One-way ANOVA was used to compare Fe concentrations between depths in the riparian soil and in the mire.

3. Results

3.1. Iron Speciation in Source Area Soils

Linear combination fitting of the XANES and EXAFS regions showed that Fe was present in riparian forest soils mainly as organically complexed Fe (SRFA), Fe oxides (modeled as ferrihydrite and goethite), and biotite (Figure 2a, Table 2). Organically complexed Fe was strongly dominant in the shallow soil 4 m from the stream (S4; 85%–91% of total Fe) and was also higher in shallower than deeper soil layers at 12 and 22 m from the stream (S12, S22). The proportion of amorphous Fe (SRFA + ferrihydrite) to crystalline Fe oxides (goethite) was higher in the shallow soil layer where there was more organically complexed Fe and in the deeper layer of S22 where ferrihydrite was abundant.

Fe speciation in the mire was notably different from that in the riparian forest soil and was much more homogenous across depths. Amorphous Fe oxides were identified as the dominant fraction (40%–61% of total Fe), with roughly equal contributions of siderite (20%–26%) and vivianite (16%–37%) (Figure 2b, Table 3). Notably, the inclusion of an organically complexed Fe model as a contributing component in the LCF fit was ineffective. The preedge peak centroid positions and intensities, which indicate the oxidation state and coordination of Fe, varied for riparian soil samples (7112.23–7113.17 eV) and mire samples (7112.62–7112.89 eV), and was consistent with a variable contribution of Fe(II) and Fe(III). In the riparian soils at S4, the contribution of Fe(II) was higher in the deeper samples, which reflects the increasing contribution of biotite and a likely redox gradient. In the mire, the DSL (200–250 cm) contained a mixture of Fe(II) and Fe(III).

3.2. Trends in Soil Solution Chemistry of Source Areas

In the riparian forest soil, which drains into the C2 stream, mean Fe concentrations in the soil solution at different depths ranged between 2.1 and 2.9 mg L^{-1} (Table S1 and Figure S1 in Supporting Information S1). While differences over depth were moderate in general, Fe concentrations at 35 cm were significantly lower than those at 45 and 55 cm ($p_{35–45}$ = 0.014, $p_{35–55}$ = 0.008). Between 2003 and 2020, Fe concentrations increased at all depths, with the highest increase within the dominant source layer (DSL, 35–55 cm), where concentrations increased by 0.23–0.26 mg L^{-1} yr^{-1} (Table S1 in Supporting Information S1, Figure 3b). DOC concentrations were more variable across depths (26–67 mg L^{-1}), with the highest concentrations in the top 10 cm and decreasing with depth (Table S1 and Figure S1 in Supporting Information S1). DOC increased at a rate of 1.41–1.90 mg L^{-1} yr^{-1} in the DSL (Figure 3d), but showed a negative trend at 25 cm and no trend at 10 cm depth (Table S1 in Supporting Information S1). SO_4^{2-} concentrations in the DSL showed a pronounced decrease in the beginning of the time

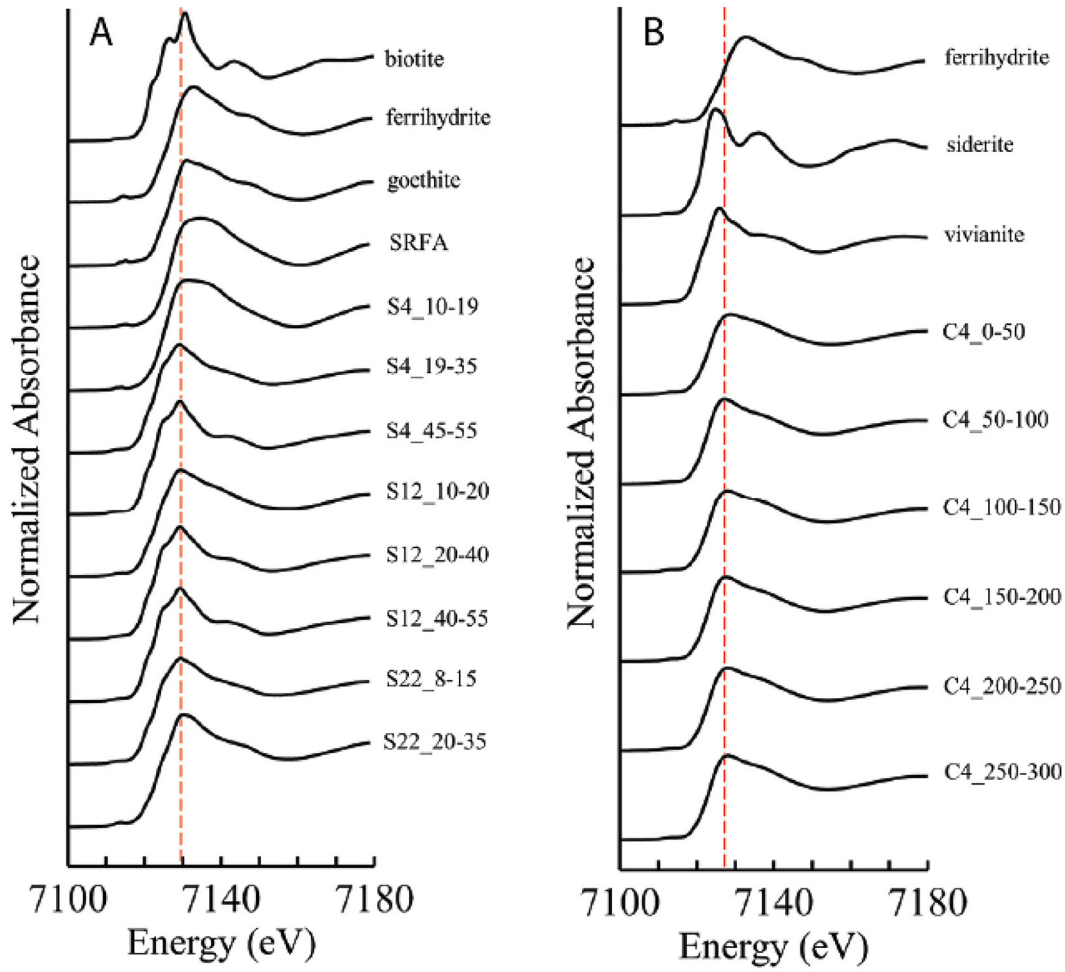

Figure 2. Normalized X-ray Absorption Near Edge Structure spectra for the riparian forest S4 soil samples (a) and the C4 mire samples (b). Standard specta are included on the top for comparison with the sample spectra (SRFA as model for organically complexed Fe). The red dashed lines serve for comparison of the peak positions.

series (2003–2006), but increased by 5-fold in 2007, and then declined gradually after that (Figure 3f). pH in the riparian soil, although measured only from 2009 to 2020, displayed no temporal trend (Figure 3h). Partial least square analysis, including data from all depths and sampling occasions, showed that Fe concentrations in riparian soil solution were negatively correlated with SO_4^{2-} (SRC = −0.30) and positively correlated with aluminum (Al; SRC = 0.24), NH^{4+} (SRC = 0.18), and DOC (SRC = 0.16) concentrations. In the DSL of the riparian zone, both Fe (tau = −0.43, $p < 0.001$) and DOC (tau = −0.38, $p < 0.001$) were strongly negatively correlated to SO_4^{2-} but not with pH.

For the mire, mean Fe concentrations in solution at different depths ranged between 0.6 and 1.8 mg L^{-1} (Figure S2 in Supporting Information S1). Fe concentrations were significantly lower in the DSL (200–250 cm), than in the layer above (150–175 cm, $p < 0.01$), but were highest at 350 cm. DOC concentrations were similar over depth, and varied from 36 to 43 mg L^{-1} (Figure S2 in Supporting Information S1). Temporal trend analysis was precluded by a large gap in the data series, but there was no apparent change in Fe concentrations when comparing the years 2004 and 2007 with 2017–2020 (Figure 4b). There was also no significant trend in DOC concentrations for the DSL in the mire ($p = 0.11$). This conforms with the data from the mire dominated stream C4, where no trends were observed for either Fe or DOC (Table 4, Figures 2a and 2c). A PLS analysis of data from the mire showed that Fe concentrations were best correlated with concentrations of other metals (SRC: Al = 0.45, silicon (Si) = 0.32, and manganese (Mn) = 0.29), while correlations with DOC (SRC = 0.06) and SO_4^{2-} (SRC = −0.06) were weak. When looking only at the DSL (200–250 cm) of the mire, Fe correlated positively with magnesium (Mg) (SRC = 0.23), DOC (SRC = 0.18), conductivity (SRC = 0.17), Al (SRC = 0.17), Mn (SRC = 0.16), and

Table 2
Proportion of Fe Phases Identified by Linear Combination Fitting and Residuals of the Fits From the X-Ray Absorption Near Edge Structure and Extended X-Ray Absorption Fine Structure Data

Distance from stream	Depth (cm)		SRFA (%)	Ferrihydrite (%)	Goethite (%)	Biotite (%)	Residuals
4 m (S4)	10–19	XANES	91	9	b.t.	b.t.	0.0000508
		EXAFS	85	15	b.t.	b.t.	0.233
	19–35	XANES	b.t.	8	61	32	0.000147
		EXAFS	b.t.	24	35	41	0.168
	45–55	XANES	b.t.	3	43	54	0.000133
		EXAFS	b.t.	6	21	73	0.257
12 m (S12)	10–20	XANES	34	8	32	27	0.0000879
		EXAFS	41	29	8	23	0.169
	20–40	XANES	b.t.	8	48	44	0.000132
		EXAFS	b.t.	11	26	63	0.650
	40–55	XANES	b.t.	6	44	51	0.000172
		EXAFS	b.t.	12	20	68	0.361
22 m (S22)	8–15	XANES	42	b.t.	14	44	0.000284
		EXAFS	31	b.t.	24	45	0.810
	20–35	XANES	18	44	13	25	0.000088
		EXAFS	14	40	20	26	0.253

Note. b.t.: below threshold. Contribution lower than the threshold limit of 1%. The soil samples were collected at different depths and distances from stream C2 in a spruce forest transect. SRFA was used as a model for organically complexed Fe.

negatively with pH (SRC = −0.11). Above the DSL at depths 125–175 cm, Fe correlated positively with other metals (SRC: Mn = 0.41, Si = 0.18, Al = 0.18), as well as DOC (SRC = 0.24) and Mg (SRC = 0.20), while the correlation with pH was negative (SRC = −0.14).

3.3. Trends in Streams Water Chemistry

Mean Fe concentrations in the streams were between 0.7 and 1.7 mg L^{-1}. Out of the 13 streams, three exhibited a significant increase in Fe for the study period (C1, C2, C7), one stream had no significant trend (C4), while the remaining nine showed significant declines in Fe concentrations (Table 4). In the forest dominated stream C2 (Figure 3a), positive Sen slopes were observed for all months of the year, with significant trends for March, April, May, June, November, and December. In the mire dominated stream C4 (Figure 4a), Sen slopes were not significant for most months, but for March and April, there were significant negative trends over time.

Significant positive trends in DOC were found in all streams except for C4, C5, and C6, which showed no significant trend (Table 4). Recovery from atmospheric sulfate (SO_4^{2-}) deposition was evident as all streams showed significant declining trends in SO_4^{2-} concentrations (Table S2 in Supporting Information S1). Significant declining trends in total nitrogen were also found for all streams except for C1, which showed no significant trend (Table S2 in Supporting Information S1). Despite the declining SO_4^{2-} concentrations, pH exhibited significantly declining trends in all streams (Table S2 in Supporting Information S1). There was no significant trend in discharge (Q) in any of the streams.

The relationship between Fe and DOC was positive in all streams, with the slope of the relationship being steeper in the lower order streams (Table S3 in Supporting Information S1). The relationship between Fe and Q showed differences between streams, with streams showing positive, negative and insignificant correlations between Fe and Q (Table S3 in Supporting Information S1). In the mire outlet stream (C4), Fe showed the strongest negative

Table 3
Proportions of Fe Phases Identified by Linear Combination Fitting Based on X-Ray Absorption Near Edge Structure Data From the Mire, and Residuals of the Fit

Depth (cm)	Ferrihydrite (%)	Siderite (%)	Vivianite (%)	Residual
00–50	61	20	19	0.000212
50–100	40	23	37	0.000187
100–150	53	24	23	0.000142
150–200	46	24	29	0.000136
200–250	56	25	19	0.000120
250–300	58	26	16	0.000144

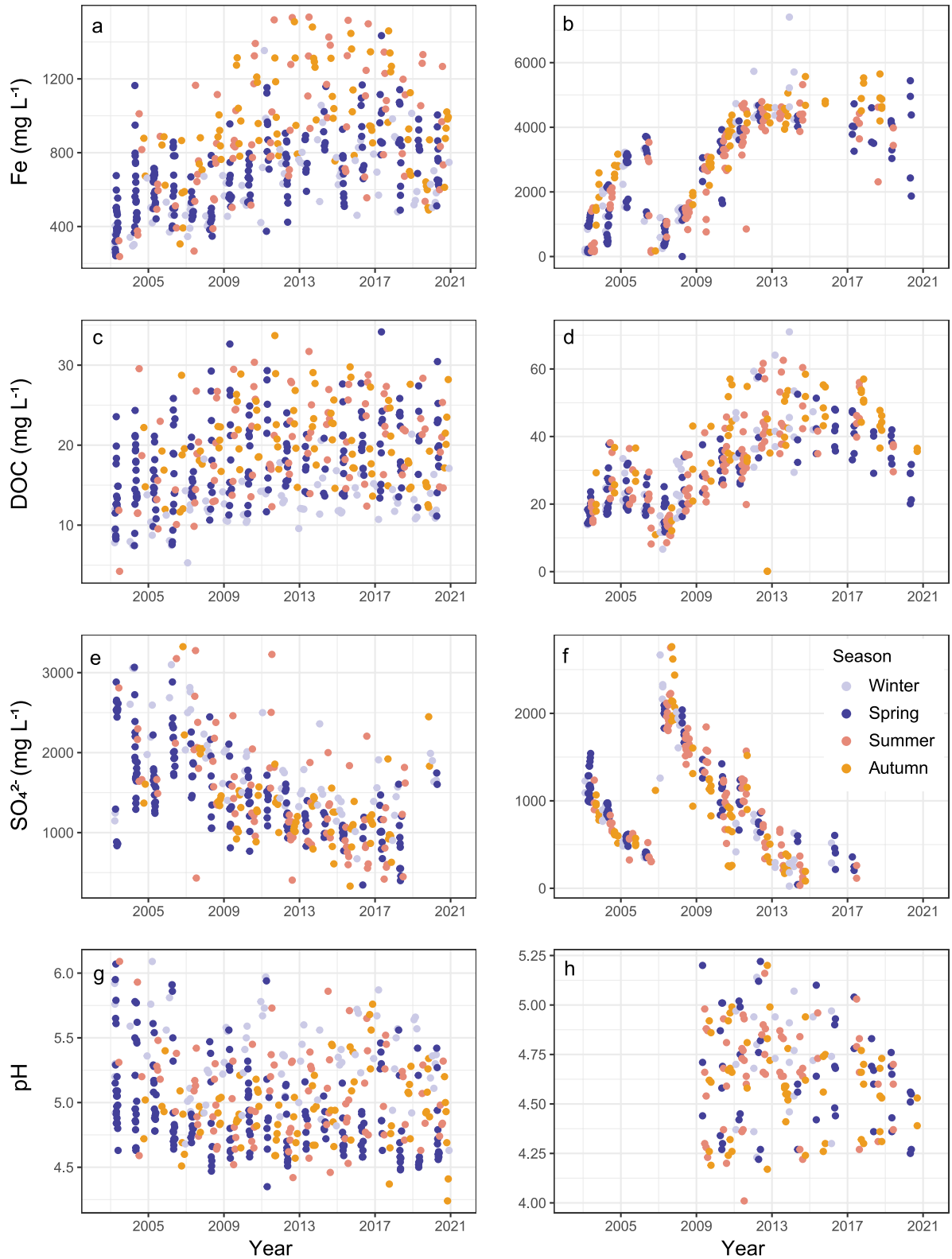

Figure 3. Fe, dissolved organic carbon, and SO_4^{2-} concentrations and pH in the forest dominated stream C2 (left panels) and in the dominant source layer (DSL, 35–55 cm) of the riparian zone (right panels, S4). Colors represent seasons: winter (December–March), spring (April–May), summer (June–August) and autumn (September–November). Statistical outliers (<5%, except for panel E (7%)) were excluded for better visualization.

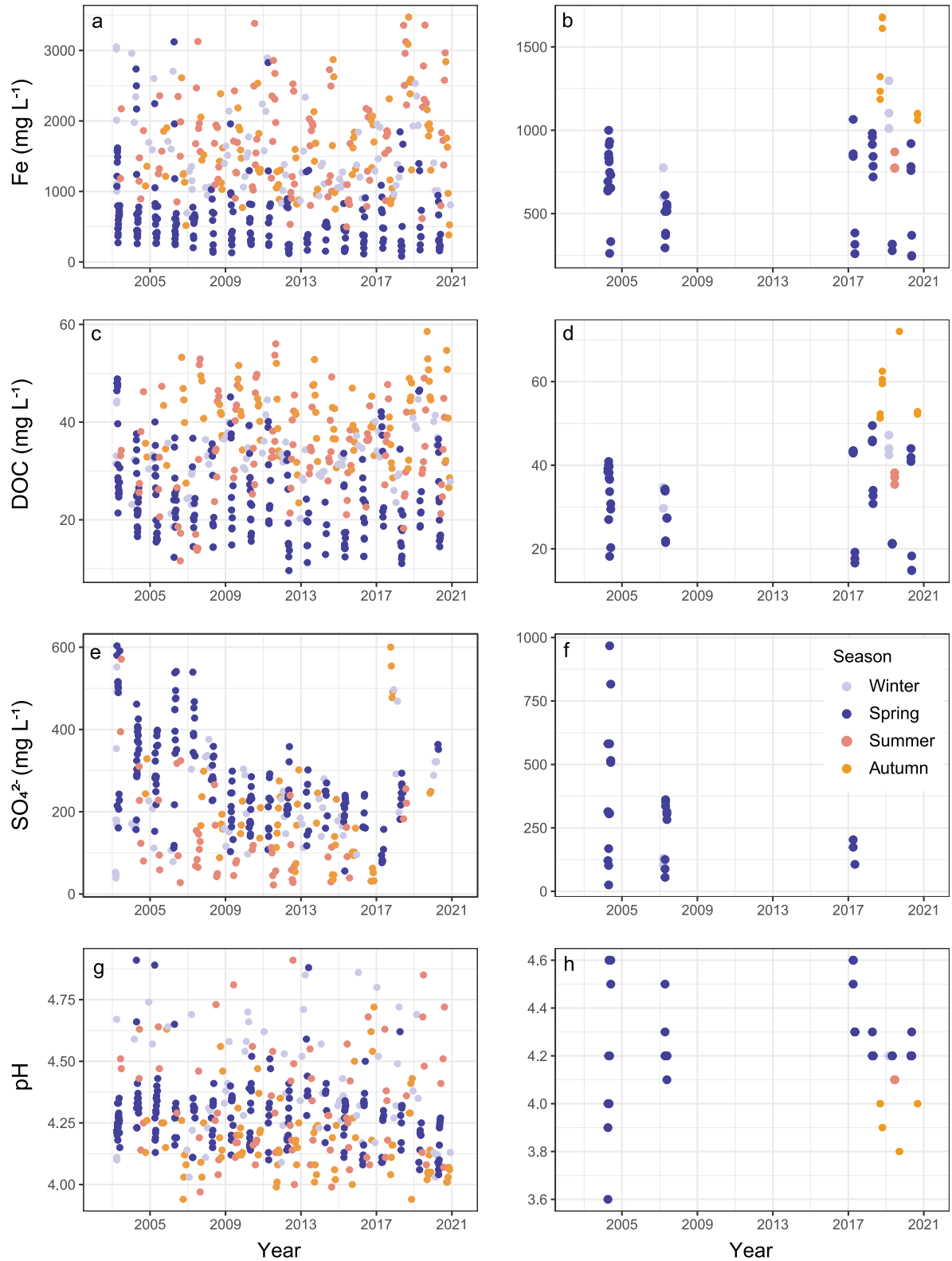

Figure 4. Fe, dissolved organic carbon, and SO_4^{2-} concentrations and pH in the mire dominated stream C4 (left panels) and in the dominant source layer (DSL, 200–250 cm) of the mire (right panels). Colors represent seasons: winter (December–March), spring (April–May), summer (June–August) and autumn (September–November). Statistical outliers (<5%, except for panels E (8%) and G (17%)) were excluded for better visualization.

Table 4
Mean Concentrations and Rates of Change for Fe and Dissolved Organic Carbon in Streams During 2003–2020

		Fe			DOC		
Stream	Stream order	Mean (mg L^{-1})	Change (mg L^{-1} y^{-1})	*p* value	Mean (mg L^{-1})	Change (mg L^{-1} y^{-1})	*p* value
C1	2	1.1	0.04	**<0.001**	19.1	0.31	**<0.001**
C2	1	0.8	0.02	**<0.001**	18.1	0.29	**<0.001**
C4	1	1.3	−0.01	0.24	31.2	−0.03	0.74
C5	1	1.7	−0.03	**<0.001**	21.4	−0.05	0.25
C6	1	1.3	−0.03	**<0.001**	17.4	0.05	0.18
C7	2	1.3	0.02	**<0.001**	23.0	0.21	**<0.001**
C9	3	1.1	−0.02	**<0.001**	16.2	0.13	**<0.01**
C10[a]	2	1.2	−0.01	**<0.05**	18.9	0.23	**<0.001**
C12[a]	3	1.3	−0.03	**<0.001**	17.6	0.20	**<0.01**
C13	3	1.3	−0.01	**<0.01**	18.6	0.28	**<0.001**
C14[a]	2	0.9	−0.03	**<0.001**	12.3	0.11	**<0.01**
C15[a]	4	0.7	−0.01	**<0.01**	11.8	0.08	**<0.05**
C16	4	1.0	−0.02	**<0.001**	10.8	0.12	**<0.01**

Note. Significant trends are in bold.
[a]Data only available for period 2003–2016.

correlation with Q, indicating the dilution at high discharge, while this relationship was positive in the forest dominated stream C2. Seasonally changing discharge also influenced Fe fluxes across the year with the highest fluxes of Fe seen during the spring freshet in April and May, while fluxes were lowest during winter baseflow (Table S4 in Supporting Information S1). Fe fluxes generally increased with catchment area.

The rate and direction of change in Fe concentrations across streams was well explained by differences in land cover (Figure 5a), that is, the Theil-Sen estimate of slope correlated positively with the integrated measure of catchment characteristics (PC1; $r^2 = 0.51$, $p = 0.015$; Kendall correlation test; Figure 5b). Catchments with high positive scores on PC1 were characterized by a higher percentage of spruce, larger tree volume, older stand

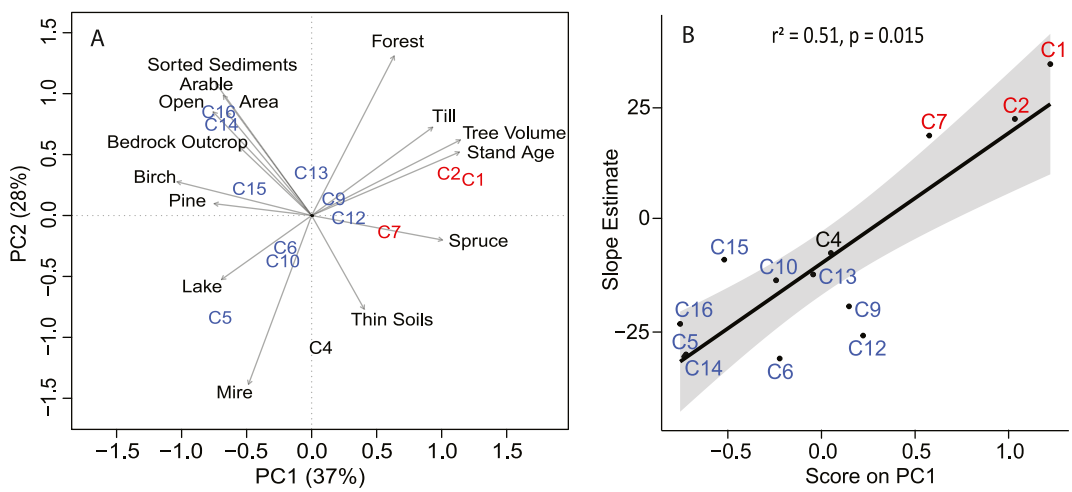

Figure 5. Distribution of the 13 streams across two principal component analysis components based on differences in catchment characteristics (a) and correlation between scores on PC1 and the Theil-Sen slopes form the Seasonal Kendall Test for Fe (b). Streams denoted in red had significant positive trends, blue had significant negative trends and black had no significant trend. The values in brackets (a) on each axis are the percentages of variance in catchment characteristics explained by each PC.

age and higher percentage of till soils in the catchment. Catchments with negative scores on PC1 had a higher proportion of birch and pine forest, open and arable land, lake and mire cover, and had a larger overall catchment size (Figure 5a).

4. Discussion

Increasing Fe concentrations have been widely reported across Northern Europe (Björnerås et al., 2017; Sarkkola et al., 2013) and while riparian soils and wetlands have been identified as major Fe sources to streams (Björkvald et al., 2008; Ingri et al., 2018), it remains unclear how these sources contribute to long-term trends. Our assessment of Fe time series across 13 nested, boreal streams provides evidence that large differences in these trends can emerge over relatively small scales as a function of catchment characteristics. Positive trends were found only in headwater streams draining catchments dominated by older spruce forests, while the remaining streams showed either no trend (a mire dominated headwater) or a significant negative trend (nine, primarily larger catchments). Consistent with the observations across the stream network, Fe concentrations increased in the spruce dominated riparian soils, while there was no evident trend in the mire peat over the 18-year study period.

In both riparian soils and forested headwater streams, Fe and DOC concentrations were well correlated, suggesting that the two are mobilized together. Surprisingly, however, the majority of streams in the network showed declining Fe trends, highlighting differences within the stream network that were not in line with increasing DOC trends observed for the majority of those streams (Fork et al., 2020). Since most sites with declining Fe trends were higher order streams, this suggests that Fe-DOC interactions alone cannot explain Fe trends downstream and that in-stream processes or changing source contributions might be driving these observations. In the following sections, we discuss our results from the standpoint of Fe movements in the catchment: starting with the soil Fe sources and mobilization into the soil solution, followed by transport into streams and finally the processing of Fe along the aquatic continuum.

4.1. Fe Mobilization From Riparian Soils

In the riparian forest soil, the contribution of Fe-OM complexes was strongly dominant in the shallow layer, where the OM content was highest, while Fe(oxy)hydroxides and biotite were more prominent in deeper soil strata. The tendency of increasing Fe(II) with soil depth may reflect biotite, which contains both Fe(II) and Fe(III) in its mineral structure. Similar speciation in the riparian soil phase was identified by Sundman et al. (2014), who also investigated speciation in the soil solution and found that it was dominated by Fe(II)-OM and Fe(III)-OM mononuclear complexes. In the present study, Fe concentrations correlated well with DOC, which is in line with Fe-OM complexes being the main form of Fe mobilized from organic riparian soils. A predominant contribution of Fe-OM complexes in the soil solution has also been found in other organic and mineral soils (Škerlep et al., 2021), highlighting the importance of OM complexation for Fe translocation and in preventing Fe precipitation (Sjöstedt et al., 2013). In addition, Fe(oxy)hydroxides can be mobilized through reductive dissolution under water-saturated periods with low oxygen conditions when Fe(III) becomes the preferred electron acceptor (Schwab & Lindsay, 1983), and through other biotic processes where Fe is dissolved by organic acids and siderophores (Reichard et al., 2007) or is dissolved to facilitate Fenton reactions (Krumina et al., 2022).

In the DSL of the riparian zone, Fe and DOC concentrations both increased during the period observed in this study and showed an inverse temporal relationship with SO_4^{2-} concentrations. Although atmospheric S deposition in Northern Sweden has largely returned to preindustrialization levels, an extreme drought in 2006 seems to have led to the oxidation of reduced organic S, causing an episodic increase in riparian soil SO_4^{2-} concentrations (Laudon, Sponseller, et al., 2021; Ledesma et al., 2016). Reduced organic S is a dominant form of S in organic soils (Skyllberg et al., 2003) and can quickly oxidize when soils are aerated during drought (Clark et al., 2005; Prietzel, Thieme, et al., 2009). We suggest that the extreme drought event led to a rapid oxidization of organic S and degradation of OM, which generated a pool of available Fe and OM that was released into solution over the following years. High SO_4^{2-} concentrations immediately after the drought likely suppressed the solubility of OM by decreasing the pH (Clark et al., 2005; Ekström et al., 2011; Evans et al., 2012), and indirectly influenced Fe, which depends on complexation with OM to remain in solution.

While SO_4^{2-} concentrations recovered to predrought levels within a couple of years, Fe and DOC continued to increase and reached concentrations twice as high as predrought. Drought induced suppression of DOC mobility

has previously been reported in peat soils, however past studies mostly report recovery to predrought DOC levels within weeks or months upon rewetting (Clark et al., 2005, 2012; Freeman et al., 2004). Yet, in a study exploring drought effects in a UK peat catchment, Worrall et al. (2006) suggest that severe drought can trigger biogeochemical processes that lead to a decade-long period of elevated DOC production. The proposed mechanism behind this is that oxygenation of organic soils triggers an enzymic latch mechanism, where enzymes are switched on by drought and are not switched off again afterward (Freeman, Evans, et al., 2001; Freeman, Ostle, & Kang, 2001). In the present study, these mechanisms could explain the decade-long increase in DOC and consequently Fe mobilization in the riparian soil and further suggest that severe drought could alter DOC and Fe trends in forested headwater streams long after such events end. Further research will be needed to explore the effects of severe droughts on riparian biogeochemistry and their potential to increase Fe and DOC mobilization (Tiwari et al., 2022).

4.2. Fe Mobilization From Mires

In the mire, poorly ordered Fe(oxy)hydroxides, siderite, and vivianite were identified as major soil phases by XAS analysis. Siderite and vivianite are known to form as authigenic secondary minerals in peat mires under anoxic conditions (Bojanowski et al., 2016; Heiberg et al., 2012; McMillan & Schwertmann, 1998). Fe(oxy)hydroxides could form as an oxidation product when Fe(II) in siderite or vivianite is oxidized. We can also not exclude that some phases, such as Fe sulfides, may have been lost due to oxidation during sample handling (Prietzel, Tyufekchieva, et al., 2009). Poorly ordered Fe(oxy)hydroxides should be available for mobilization by reductive dissolution, which has been shown to be an important process controlling Fe mobility in wetlands (Knorr, 2013; Roden & Wetzel, 2002); however, oxidation could also lead to the release of Fe from vivianite or siderite. In this study, the PLS analysis showed a strong positive correlation between Fe and Mn in the mire, especially above the DSL, indicating that reductive dissolution plays an important role in Fe mobilization in the mire. Since Mn is reduced at higher redox potentials than Fe, we can assume that when conditions favor Fe reduction, Mn will also be reduced and there will be a positive correlation between the two in solution (Shiller, 1997). Changing redox conditions during water table fluctuations have previously been shown to be important in Fe mobilization from wetlands (Knorr, 2013). In the present study, drought likely had little effect on Fe exports from the mire since the DSL is located several meters deep and is unlikely to get oxidized during even extreme drought events. In shallower layers of the mire, extreme drought could lead to similar mobilization of Fe and DOC as discussed for riparian soils, but we were unable to observe this due to the lack of continuous soil solution data.

4.3. From Sources to Streams

Previous studies testing surface water Fe trends in Northern Europe have mostly reported increasing concentrations (Kritzberg & Ekström, 2012; Sarkkola et al., 2013; Xiao & Riise, 2021), while decreasing trends have been reported in some parts of North America (Björnerås et al., 2017). Here we observe these opposing trends within a single nested mesoscale catchment. The fact that streams with increasing Fe trends in this study were dominated by coniferous forest conforms with an analysis on a much wider geographic scale, demonstrating that rates of increasing Fe concentrations were higher in catchments with a larger proportion of coniferous forest (Björnerås et al., 2017). In older spruce forests, thick organic soil layers accumulate (Rosenqvist et al., 2010) and can support high concentrations of Fe-OM complexes in solution (Škerlep et al., 2021). The accumulation of OM is particularly pronounced in riparian zones, which has been identified as significant contributors of Fe to boreal streams (Ingri et al., 2018). On the other hand, mire Fe concentrations did not change for the duration of this study, which was reflected in the stream (C4) that directly drains the mire. While hydrological conditions may exert strong seasonal controls on Fe concentrations coming from the mire (Björkvald et al., 2008), discharge showed no long-term trend. Surprisingly, stream C5, which is located directly at a lake outlet, had the highest average Fe concentrations and showed a declining Fe trend. Collectively, these observations show how catchment heterogeneity, namely the relative cover of forests, mires, and lakes, can regulate Fe dynamics in headwater streams, in this case leading to highly variable trends across relatively small spatial scales.

While Fe concentrations in streams reflect changes in the terrestrial sources, we show that changes in the headwaters cannot be generalized to higher-order streams in the same network. Indeed, the declining Fe concentrations in nine of the streams were unexpected, not least considering that DOC concentrations were increasing in the majority of streams (10 out of 13; Table 4; Fork et al. (2020)). Fe and DOC concentra-

tions in boreal headwater streams are usually well correlated (Neubauer et al., 2013; Oni et al., 2013), both because the major source for both is organic soils, and because organically complexed Fe appears to be the dominant form of Fe transported from soils to headwaters (Herzog et al., 2020; Sjöstedt et al., 2013; Sundman et al., 2014). Despite these interrelationships, our results suggest that while increases in DOC input to headwaters can translate into browning throughout the network, the upstream-downstream Fe trends are seemingly uncoupled. This uncoupling could arise from ongoing changes in in-stream Fe processing or if headwater Fe trends from particular sources contribute to higher relative signals downstream. For example, an explanation for declining Fe trends at some of these sites could be that the lake outlet at C5 dominated Fe loadings to sites further downstream, since it had the highest average Fe concentrations and showed a long-term decline in Fe. The lake outlet (C5) has been shown to contribute up to 75%, 50%, and 25% of the total water flow to streams C6, C9, and C13, respectively, and has the highest downstream water flow contribution during moderate flow levels (Leach & Laudon, 2019). This hypothesis is further supported by our calculations of Fe fluxes, which show that during some periods of the year, C5 represented up to 85%, 49% and 21% of the Fe loadings at C6, C9, and C13, respectively (Table S4 in Supporting Information S1). Declining Fe concentrations in the lake would therefore lead to declining trends at its outlet C5 as well as at downstream locations C6, C9, and C13. The lake is small (0.04 km2) but deep enough (maximum depth 6.7 m) to allow the loss of Fe by sedimentation, which may increase during drier periods when retention time in the lake increases (Weyhenmeyer et al., 2014). Unfortunately, long-term physio-chemical data were not available for the lake and the stream data could not help pinpoint mechanisms diving downstream Fe concentration trends. The decline could be connected to processing in the water column, where for example, pH or light induced transformations of Fe leads to aggregation and loss from suspension (Neubauer et al., 2013; Weyhenmeyer et al., 2014). Alternatively, the declining trends could be caused by changing climate (e.g., cloud cover, ice cover, water temperature, stratification) or changing metabolism in the water column. Regardless of the mechanisms behind observed Fe trends, hydrological connectivity between catchment sources and streams exerts a strong control over stream Fe concentrations and can have a strong downstream influence. To explain downstream trends when headwater trends are heterogenous, it is clearly important to understand how water from the smallest streams mixes, as well as how the pot contribution from groundwater sources may further alter chemical signals (Leach & Laudon, 2019).

5. Conclusions

Organic soils are major sources of Fe to boreal freshwaters, and in this study, we show that forested parts of catchments contributed to increasing Fe trends, while mires did not seem to be increasing sources. While large-scale drivers such as atmospheric deposition and climate change might explain Fe trends on regional and large catchment scales (Björnerås et al., 2017), we show that when studying headwater streams, understanding the contributions from discrete catchment sources is essential. This is highlighted by the differential trends in streams draining forest-, mire-, and lake-dominated catchments in this study. At the same time, we show that changes in headwater Fe concentrations cannot necessarily be generalized to higher order streams downstream. Although we show that Fe and DOC are strongly correlated with headwater streams, the mismatch in long-term trends suggests that changes in DOC concentrations alone cannot explain the trends in Fe concentrations. Finally, we show that extreme events such as drought can shape soil solution and stream Fe dynamics not only within a season but also over a span of several years and can strongly influence long-term trends. Although it is unclear how climate change will shape the frequency and severity of droughts in northern regions (Forzieri et al., 2014; Spinoni et al., 2018), understanding their effects on Fe and other OM associated metals will be important in predicting future stream water chemistry trajectories. Further studies are needed to investigate the exact mechanisms behind the drought induced release of Fe and DOC from organic soils and how these processes will affect stream Fe dynamics in diverse catchments.

Data Availability Statement

The data used for the purpose of this study are available through zenodo.org via https://doi.ogr/10.5281/zenodo.7374175 and can be freely accessed at https://zenodo.org/record/7374175#.Y4UdKXbMIaY Škerlep et al. (2022).

Acknowledgments
We would like to acknowledge Svenska Forskningsrådet Formas (2019-00889) for providing funds for the project and Carl Tryggers Stiftelse (CTS20:407). We also acknowledge financial support for the Krycklan Catchment Study, including the Swedish Science Foundation (VR), Swedish Infrastructure for Ecosystem Science (SITES), the VR extreme event project, Future Forests, the Kempe Foundation, the Swedish Research Council for Sustainable Development (FORMAS), European Union's Horizon 2020 Research and Innovation Programme under the Marie Sklodowska-Curie Grant Agreement No 734317 (HiFreq), KAW (Branch Point program), and the Swedish Nuclear Waste Company (SKB). We also acknowledge the work of KCS technicians who collected and processed the samples that comprise these long-term records. For the synchrotron data, we acknowledge MAX IV Laboratory for time on Beamline Balder under Proposal 20200018. Research conducted at MAX IV, a Swedish national user facility, is supported by the Swedish Research council under contract 2018-07152, the Swedish Governmental Agency for Innovation Systems under contract 2018-04969, and Formas under contract 2019-02496. Additional synchrotron work was conducted at beamline line 4-1 at the Stanford Synchrotron Radiation Lightsource (SSRL), California, USA. The use of the Stanford Synchrotron Radiation Lightsource, SLAC National Accelerator Laboratory, is supported by the U.S. Department of Energy, Office of Science, Office of Basic Energy Sciences under Contract DE-AC02-76SF00515. The SSRL Structural Molecular Biology Program is supported by the DOE Office of Biological and Environmental Research and by the National Institutes of Health, National Institute of General Medical Sciences (including P41GM103393). The contents of this publication are solely the responsibility of the authors and do not necessarily represent the official views of NIGMS or NIH.

References

Björkvald, L., Buffam, I., Laudon, H., & Mörth, C.-M. (2008). Hydrogeochemistry of Fe and Mn in small boreal streams: The role of seasonality, landscape type and scale. *Geochimica et Cosmochimica Acta*, *72*(12), 2789–2804. https://doi.org/10.1016/j.gca.2008.03.024

Björnerås, C., Weyhenmeyer, G. A., Evans, C. D., Gessner, M. O., Grossart, H. P., Kangur, K., et al. (2017). Widespread increases in iron concentration in European and North American freshwaters. *Global Biogeochemical Cycles*, *31*(10), 1488–1500. https://doi.org/10.1002/2017gb005749

Björnerås, C., Weyhenmeyer, G. A., Hammarlund, D., Persson, P., & Kritzberg, E. S. (2022). Sediment records shed light on drivers of decadal iron concentration increase in a Boreal Lake. *Journal of Geophysical Research: Biogeosciences*, *127*(3), e2021JG006670. https://doi.org/10.1029/2021jg006670

Bojanowski, M. J., Jaroszewicz, E., Košir, A., Łoziński, M., Marynowski, L., Wysocka, A., & Derkowski, A. (2016). Root-related rhodochrosite and concretionary siderite formation in oxygen-deficient conditions induced by a ground-water table rise. *Sedimentology*, *63*(3), 523–551. https://doi.org/10.1111/sed.12227

Clark, J., Heinemeyer, A., Martin, P., & Bottrell, S. (2012). Processes controlling DOC in pore water during simulated drought cycles in six different UK peats. *Biogeochemistry*, *109*(1), 253–270. https://doi.org/10.1007/s10533-011-9624-9

Clark, J. M., Chapman, P. J., Adamson, J. K., & Lane, S. N. (2005). Influence of drought-induced acidification on the mobility of dissolved organic carbon in peat soils. *Global Change Biology*, *11*(5), 791–809. https://doi.org/10.1111/j.1365-2486.2005.00937.x

Ekström, S. M., Regnell, O., Reader, H. E., Nilsson, P. A., Löfgren, S., & Kritzberg, E. S. (2016). Increasing concentrations of iron in surface waters as a consequence of reducing conditions in the catchment area. *Journal of Geophysical Research: Biogeosciences*, *121*(2), 479–493. https://doi.org/10.1002/2015jg003141

Ekström, S. M., Kritzberg, E. S., Kleja, D. B., Larsson, N., Nilsson, P. A., Graneli, W., & Bergkvist, B. (2011). Effect of acid deposition on quantity and quality of dissolved organic matter in soil–water. *Environmental Science & Technology*, *45*(11), 4733–4739. https://doi.org/10.1021/es104126f

Evans, C. D., Jones, T. G., Burden, A., Ostle, N., Zielinski, P., Cooper, M. D. A., et al. (2012). Acidity controls on dissolved organic carbon mobility in organic soils. *Global Change Biology*, *18*(11), 3317–3331. https://doi.org/10.1111/j.1365-2486.2012.02794.x

Fork, M. L., Sponseller, R. A., & Laudon, H. (2020). Changing source-transport dynamics drive differential browning trends in a boreal stream network. *Water Resources Research*, *56*(2), e2019WR026336. https://doi.org/10.1029/2019wr026336

Forzieri, G., Feyen, L., Rojas, R., Flörke, M., Wimmer, F., & Bianchi, A. (2014). Ensemble projections of future streamflow droughts in Europe. *Hydrology and Earth System Sciences*, *18*(1), 85–108. https://doi.org/10.5194/hess-18-85-2014

Freeman, C., Evans, C., Monteith, D., Reynolds, B., & Fenner, N. (2001). Export of organic carbon from peat soils. *Nature*, *412*(6849), 785. https://doi.org/10.1038/35090628

Freeman, C., Fenner, N., Ostle, N., Kang, H., Dowrick, D., Reynolds, B., et al. (2004). Export of dissolved organic carbon from peatlands under elevated carbon dioxide levels. *Nature*, *430*(6996), 195–198. https://doi.org/10.1038/nature02707

Freeman, C., Ostle, N., & Kang, H. (2001). An enzymic'latch'on a global carbon store. *Nature*, *409*(6817), 149. https://doi.org/10.1038/35051650

Fuchs, R., Herold, M., Verburg, P. H., & Clevers, J. G. P. W. (2013). A high-resolution and harmonized model approach for reconstructing and analysing historic land changes in Europe. *Biogeosciences*, *10*(3), 1543–1559. https://doi.org/10.5194/bg-10-1543-2013

George, G. N., & Pickering, I. J. (2000). *Exafspak & Edg_Fit*. Menlo Park, USA: Stanford Synchrotron Radiation Lightsource.

Grabs, T., Bishop, K., Laudon, H., Lyon, S. W., & Seibert, J. (2012). Riparian zone hydrology and soil water total organic carbon (TOC): Implications for spatial variability and upscaling of lateral riparian TOC exports. *Biogeosciences*, *9*(10), 3901–3916. https://doi.org/10.5194/bg-9-3901-2012

Haaland, S., Hongve, D., Laudon, H., Riise, G., & Vogt, R. D. (2010). Quantifying the drivers of the increasing colored organic matter in boreal surface waters. *Environmental Science & Technology*, *44*(8), 2975–2980. https://doi.org/10.1021/es903179j

Heiberg, L., Koch, C. B., Kjaergaard, C., Jensen, H. S., & Hansen, H. C. B. (2012). Vivianite precipitation and phosphate sorption following iron reduction in anoxic soils. *Journal of Environmental Quality*, *41*(3), 938–949. https://doi.org/10.2134/jeq2011.0067

Herzog, S. D., Persson, P., Kvashnina, K., & Kritzberg, E. S. (2020). Organic iron complexes enhance iron transport capacity along estuarine salinity gradients of Baltic estuaries. *Biogeosciences*, *17*(2), 331–344. https://doi.org/10.5194/bg-17-331-2020

Hirsch, R. M., & Slack, J. R. (1984). A nonparametric trend test for seasonal data with serial dependence. *Water Resources Research*, *20*(6), 727–732. https://doi.org/10.1029/wr020i006p00727

Ingri, J., Conrad, S., Lidman, F., Nordblad, F., Engström, E., Rodushkin, I., & Porcelli, D. (2018). Iron isotope pathways in the boreal landscape: Role of the riparian zone. *Geochimica et Cosmochimica Acta*, *239*, 49–60. https://doi.org/10.1016/j.gca.2018.07.030

Karlsen, R. H., Bishop, K., Grabs, T., Ottosson-Löfvenius, M., Laudon, H., & Seibert, J. (2019). The role of landscape properties, storage and evapotranspiration on variability in streamflow recessions in a boreal catchment. *Journal of Hydrology*, *570*, 315–328. https://doi.org/10.1016/j.jhydrol.2018.12.065

Karlsen, R. H., Grabs, T., Bishop, K., Buffam, I., Laudon, H., & Seibert, J. (2016). Landscape controls on spatiotemporal discharge variability in a boreal catchment. *Water Resources Research*, *52*(8), 6541–6556. https://doi.org/10.1002/2016wr019186

Karlsson, T., & Persson, P. (2012). Complexes with aquatic organic matter suppress hydrolysis and precipitation of Fe (III). *Chemical Geology*, *322*, 19–27. https://doi.org/10.1016/j.chemgeo.2012.06.003

Klementiev, K. (2001). VIPER for windows. *Journal of Physics D Applied Physics*, *34*(2), 209–217.

Knorr, K. H. (2013). DOC-dynamics in a small headwater catchment as driven by redox fluctuations and hydrological flow paths—Are DOC exports mediated by iron reduction/oxidation cycles? *Biogeosciences*, *10*(2), 891–904. https://doi.org/10.5194/bg-10-891-2013

Kritzberg, E., & Ekström, S. (2012). Increasing iron concentrations in surface waters–a factor behind brownification? *Biogeosciences*, *9*(4), 1465–1478. https://doi.org/10.5194/bg-9-1465-2012

Kritzberg, E. S. (2017). Centennial-long trends of lake browning show major effect of afforestation. *Limnology and Oceanography Letters*, *2*(4), 105–112. https://doi.org/10.1002/lol2.10041

Kritzberg, E. S., Hasselquist, E. M., Škerlep, M., Löfgren, S., Olsson, O., Stadmark, J., et al. (2019). Browning of freshwaters: Consequences to ecosystem services, underlying drivers, and potential mitigation measures. *Ambio*, *49*(2), 1–16. https://doi.org/10.1007/s13280-019-01227-5

Krumina, L., Op De Beeck, M., Meklesh, V., Tunlid, A., & Persson, P. (2022). Ectomycorrhizal fungal transformation of dissolved organic matter: Consequences for reductive iron oxide dissolution and Fenton-based oxidation of mineral-associated organic matter. *Frontiers of Earth Science*, *654*. https://doi.org/10.3389/feart.2022.763695

Laudon, H., Hasselquist, E. M., Peichl, M., Lindgren, K., Sponseller, R., Lidman, F., et al. (2021). Northern landscapes in transition: Evidence, approach and ways forward using the Krycklan Catchment Study. *Hydrological Processes*, *35*(4), e14170. https://doi.org/10.1002/hyp.14170

Laudon, H., Seibert, J., Köhler, S., & Bishop, K. (2004). Hydrological flow paths during snowmelt: Congruence between hydrometric measurements and oxygen 18 in meltwater, soil water, and runoff. *Water Resources Research*, *40*(3), W03102. https://doi.org/10.1029/2003wr002455

Laudon, H., Sponseller, R. A., & Bishop, K. (2021). From legacy effects of acid deposition in boreal streams to future environmental threats. *Environmental Research Letters*, *16*(1), 015007. https://doi.org/10.1088/1748-9326/abd064

Laudon, H., Taberman, I., Agren, A., Futter, M., Ottosson-Lofvenius, M., & Bishop, K. (2013). The Krycklan Catchment Study-A flagship infrastructure for hydrology, biogeochemistry, and climate research in the boreal landscape. *Water Resources Research*, *49*(10), 7154–7158. https://doi.org/10.1002/wrcr.20520

Leach, J. A., & Laudon, H. (2019). Headwater lakes and their influence on downstream discharge. *Limnology and Oceanography Letters*, *4*(4), 105–112. https://doi.org/10.1002/lol2.10110

Ledesma, J. L. J., Futter, M. N., Laudon, H., Evans, C. D., & Kohler, S. J. (2016). Boreal forest riparian zones regulate stream sulfate and dissolved organic carbon. *Science of the Total Environment*, *560*, 110–122. https://doi.org/10.1016/j.scitotenv.2016.03.230

Lidman, F., Boily, Å., Laudon, H., & Köhler, S. J. (2017). From soil water to surface water—How the riparian zone controls element transport from a boreal forest to a stream. *Biogeosciences*, *14*(12), 3001–3014. https://doi.org/10.5194/bg-14-3001-2017

Lindbladh, M., Axelsson, A.-L., Hultberg, T., Brunet, J., & Felton, A. (2014). From broadleaves to spruce—The borealization of southern Sweden. *Scandinavian Journal of Forest Research*, *29*(7), 686–696. https://doi.org/10.1080/02827581.2014.960893

Maranger, R., Canham, C. D., Pace, M. L., & Papaik, M. J. (2006). A spatially explicit model of iron loading to lakes. *Limnology & Oceanography*, *51*(1), 247–256. https://doi.org/10.4319/lo.2006.51.1.0247

Marchetto, A., & Marchetto, M. A. (2015). Package "rkt". *Technology*, *40*, 4066–4073.

McMillan, S., & Schwertmann, U. (1998). Morphological and genetic relations between siderite, calcite and goethite in a Low Moor Peat from southern Germany. *European Journal of Soil Science*, *49*(2), 283–293. https://doi.org/10.1046/j.1365-2389.1998.00154.x

Monteith, D. T., Henrys, P. A., Evans, C. D., Malcolm, I., Shilland, E. M., & Pereira, M. (2015). Spatial controls on dissolved organic carbon in upland waters inferred from a simple statistical model. *Biogeochemistry*, *123*(3), 363–377. https://doi.org/10.1007/s10533-015-0071-x

Monteith, D. T., Stoddard, J. L., Evans, C. D., de Wit, H. A., Forsius, M., Hogasen, T., et al. (2007). Dissolved organic carbon trends resulting from changes in atmospheric deposition chemistry. *Nature*, *450*(7169), 537–540. https://doi.org/10.1038/nature06316

Musolff, A., Selle, B., Büttner, O., Opitz, M., & Tittel, J. (2017). Unexpected release of phosphate and organic carbon to streams linked to declining nitrogen depositions. *Global Change Biology*, *23*(5), 1891–1901. https://doi.org/10.1111/gcb.13498

Neal, C., Lofts, S., Evans, C., Reynolds, B., Tipping, E., & Neal, M. (2008). Increasing iron concentrations in UK upland waters. *Aquatic Geochemistry*, *14*(3), 263–288. https://doi.org/10.1007/s10498-008-9036-1

Neubauer, E., Köhler, S. J., von der Kammer, F., Laudon, H., & Hofmann, T. (2013). Effect of pH and stream order on iron and arsenic speciation in boreal catchments. *Environmental Science & Technology*, *47*(13), 7120–7128. https://doi.org/10.1021/es401193j

Oksanen, J., Blanchet, F. G., Kindt, R., Legendre, P., Minchin, P. R., O'hara, R., et al. (2013). Package "vegan". Community ecology package, version. (Vol. 2, pp. 1–295).

Oni, S. K., Futter, M. N., Bishop, K., Köhler, S. J., Ottosson-Löfvenius, M., & Laudon, H. (2013). Long-term patterns in dissolved organic carbon, major elements and trace metals in boreal headwater catchments: Trends, mechanisms and heterogeneity. *Biogeosciences*, *10*(4), 2315–2330. https://doi.org/10.5194/bg-10-2315-2013

Palviainen, M., Lehtoranta, J., Ekholm, P., Ruoho-Airola, T., & Kortelainen, P. (2015). Land cover controls the export of terminal electron acceptors from boreal catchments. *Ecosystems*, *18*(2), 343–358. https://doi.org/10.1007/s10021-014-9832-y

Peralta-Tapia, A., Sponseller, R. A., Tetzlaff, D., Soulsby, C., & Laudon, H. (2015). Connecting precipitation inputs and soil flow pathways to stream water in contrasting boreal catchments. *Hydrological Processes*, *29*(16), 3546–3555. https://doi.org/10.1002/hyp.10300

Prietzel, J., Thieme, J., Tyufekchieva, N., Paterson, D., McNulty, I., & Kögel-Knabner, I. (2009a). Sulfur speciation in well-aerated and wetland soils in a forested catchment assessed by sulfur K-edge X-ray absorption near-edge spectroscopy (XANES). *Journal of Plant Nutrition and Soil Science*, *172*(3), 393–403. https://doi.org/10.1002/jpln.200800054

Prietzel, J., Tyufekchieva, N., Eusterhues, K., Kögel-Knabner, I., Thieme, J., Paterson, D., et al. (2009b). Anoxic versus oxic sample pretreatment: Effects on the speciation of sulfur and iron in well-aerated and wetland soils as assessed by X-ray absorption near-edge spectroscopy (XANES). *Geoderma*, *153*(3–4), 318–330. https://doi.org/10.1016/j.geoderma.2009.08.015

Reichard, P., Kretzschmar, R., & Kraemer, S. M. (2007). Dissolution mechanisms of goethite in the presence of siderophores and organic acids. *Geochimica et Cosmochimica Acta*, *71*(23), 5635–5650. https://doi.org/10.1016/j.gca.2006.12.022

Roden, E. E., & Wetzel, R. G. (2002). Kinetics of microbial Fe (III) oxide reduction in freshwater wetland sediments. *Limnology & Oceanography*, *47*(1), 198–211. https://doi.org/10.4319/lo.2002.47.1.0198

Rosenqvist, L., Kleja, D. B., & Johansson, M. B. (2010). Concentrations and fluxes of dissolved organic carbon and nitrogen in a Picea abies chronosequence on former arable land in Sweden. *Forest Ecology and Management*, *259*(3), 275–285. https://doi.org/10.1016/j.foreco.2009.10.013

Sanchez, G., & Sanchez, M. G. (2012). Package "plsdepot" partial least squares (PLS) data analysis methods, v. 0.1. (p. 17).

Sarkkola, S., Nieminen, M., Koivusalo, H., Lauren, A., Kortelainen, P., Mattsson, T., et al. (2013). Iron concentrations are increasing in surface waters from forested headwater catchments in eastern Finland. *Science of the Total Environment*, *463–464*, 683–689. https://doi.org/10.1016/j.scitotenv.2013.06.072

Schwab, A., & Lindsay, W. (1983). Effect of redox on the solubility and availability of iron. *Soil Science Society of America Journal*, *47*(2), 201–205. https://doi.org/10.2136/sssaj1983.03615995004700020005x

Shiller, A. M. (1997). Dissolved trace elements in the Mississippi river: Seasonal, interannual, and decadal variability. *Geochimica et Cosmochimica Acta*, *61*(20), 4321–4330. https://doi.org/10.1016/s0016-7037(97)00245-7

Sjöstedt, C., Persson, I., Hesterberg, D., Kleja, D. B., Borg, H., & Gustafsson, J. P. (2013). Iron speciation in soft-water lakes and soils as determined by EXAFS spectroscopy and geochemical modelling. *Geochimica et Cosmochimica Acta*, *105*, 172–186. https://doi.org/10.1016/j.gca.2012.11.035

Škerlep, M., Nehzati, S., Johansson, U., Kleja, D. B., Persson, P., & Kritzberg, E. S. (2021). Spruce forest afforestation leading to increased Fe mobilization from soils. *Biogeochemistry*, *157*(3), 1–18. https://doi.org/10.1007/s10533-021-00874-9

Škerlep, M., Nehzati, S., Sponseller, R. A., Persson, P., Laudon, H., & Kritzberg, E. S. (2022). Skerlep et al. DATA Differential trends in iron concentrations of boreal streams linked to catchment characteristics. (Version 1) [Dataset]. Zenodo. https://doi.org/10.5281/zenodo.6617139

Skyllberg, U., Qian, J., Frech, W., Xia, K., & Bleam, W. F. (2003). Distribution of mercury, methyl mercury and organic sulphur species in soil, soil solution and stream of a boreal forest catchment. *Biogeochemistry*, *64*(1), 53–76. https://doi.org/10.1023/a:1024904502633

Solomon, C. T., Jones, S. E., Weidel, B. C., Buffam, I., Fork, M. L., Karlsson, J., et al. (2015). Ecosystem consequences of changing inputs of terrestrial dissolved organic matter to lakes: Current knowledge and future challenges. *Ecosystems*, *18*(3), 376–389. https://doi.org/10.1007/s10021-015-9848-y

Spinoni, J., Vogt, J. V., Naumann, G., Barbosa, P., & Dosio, A. (2018). Will drought events become more frequent and severe in Europe? *International Journal of Climatology*, *38*(4), 1718–1736. https://doi.org/10.1002/joc.5291

Stumm, W., & Morgan, J. J. (2012). *Aquatic chemistry: Chemical equilibria and rates in natural waters*. (Vol. 126). John Wiley & Sons.

Sundman, A., Karlsson, T., Laudon, H., & Persson, P. (2014). XAS study of iron speciation in soils and waters from a boreal catchment. *Chemical Geology*, *364*, 93–102. https://doi.org/10.1016/j.chemgeo.2013.11.023

Tiwari, T., Sponseller, R. A., & Laudon, H. (2022). The emerging role of drought as a regulator of dissolved organic carbon in boreal landscapes. *Nature Communications*, *13*(1), 1–11. https://doi.org/10.1038/s41467-022-32839-3

Weyhenmeyer, G. A., Prairie, Y. T., & Tranvik, L. J. (2014). Browning of boreal freshwaters coupled to carbon-iron interactions along the aquatic continuum. *PLoS One*, *9*(2), e88104. https://doi.org/10.1371/journal.pone.0088104

Wilke, M., Farges, F., Petit, P.-E., Brown, G. E., Jr., & Martin, F. (2001). Oxidation state and coordination of Fe in minerals: An Fe K-XANES spectroscopic study. *American Mineralogist*, *86*(5–6), 714–730. https://doi.org/10.2138/am-2001-5-612

Wojdyr, M. (2010). Fityk: A general-purpose peak fitting program. *Journal of Applied Crystallography*, *43*(5-1), 1126–1128. https://doi.org/10.1107/s0021889810030499

Worrall, F., Burt, T., & Adamson, J. (2006). Trends in drought frequency–the fate of DOC export from British peatlands. *Climatic Change*, *76*(3), 339–359. https://doi.org/10.1007/s10584-006-9069-7

Xiao, Y., & Riise, G. (2021). Coupling between increased lake color and iron in boreal lakes. *Science of the Total Environment*, *767*, 145104. https://doi.org/10.1016/j.scitotenv.2021.145104